ISIJ International, Vol. 51 (2011), No. 4, pp. 645–650

Development and Characterization of a New Type of Ductile Iron with a Novel Multi-phase Microstructure

Mayra LAGARDE, Alejandro BASSO, Ricardo Cesar DOMMARCO and Jorge SIKORA

Faculty of Engineering. INTEMA. National University of Mar del Plata. CONICET, Av. Juan B. Justo 4302, (B7608FDQ) Mar del Plata, Argentina. E-mail: abasso@fi.mdp.edu.ar

(*Received on August 11, 2010; accepted on December 21, 2010*)

Over the last few years two new types of Ductile Iron (DI) have been developed based on Austempered DI (ADI), called Dual Phase ADI and Carbidic ADI (CADI), respectively. In the light of the experience acquired when studying these DI variants, the authors found motivating the possibility of obtaining a new type of multi-phase DI (MPDI), combining their main microstructural characteristics. A DI melt alloyed with 2%Cr, exhibiting free carbides and a pearlitic matrix in its as-cast condition, was used. The upper (U_{CT}) and lower (L_{CT}) critical temperatures of the Fe–C–Si equilibrium diagram region, where ferrite (α), austenite (γ) and graphite (Gr) coexist (called "intercritical interval"), were determined by heat treatment and microstructural analysis on samples previously annealed. Carbides stability was studied, and its dissolution was found to be negligible. It was possible to obtain free or allotriomorphic ferrite and austenite by isothermal austenitizing at temperatures within the intercritical interval, and then transform the remaining austenite into ausferrite after an austempering step. Therefore, multi- phase microstructures composed of graphite nodules, free carbides, free ferrite and ausferrite were obtained. The possibility of obtaining MPDI directly from the as-cast structure was also analyzed, and it was found that very similar microstructures to those previously annealed can be obtained by austenitizing samples at the same temperature range. These results proved that the pearlite → austenite transformation kinetics is rapid, as it took only one hour for the transformation to occur.

KEY WORDS: ductile iron; ADI; multi-phase microstructure; ausferrite; ferrite; carbides.

1. Introduction

Ever since its discovery in the early 40's, Ductile Iron (DI) has extended notoriously its field of application due to the benefits which cast manufacturing provides. DI has also turned production more economical and speedy, and made a wide range of mechanical and technological properties available. In spite of this, research efforts are still being devoted to DI, leading to some of the latest advances in the development of carbidic austempered ductile iron (CADI) and dual phase austempered ductile iron (dual phase ADI).

Carbidic Austempered Ductile Iron (CADI). Most industrial machine parts are exposed to wear. Considering the volume of material lost,[1] abrasion is the main wear mechanism, and abrasion wear is generally associated to mining, construction and agricultural industries.

Needles to say, some ADI variants feature not only high strength and toughness properties, but also very good abrasive wear resistance, when compared to steels. It has been documented that ADI behaves satisfactorily under low and high stress abrasion when heat treatment parameters are properly selected.[2,3] Furthermore, regarding heavy abrasive conditions, a new type of ADI containing free carbides (CADI) has recently burst into the market.[4,5] The presence of carbides reinforces the matrix against abrasive particles penetration, reducing impact toughness at the same time.[4–6]

Carbide precipitation concerning CADI production can be promoted in different ways, such as by controlling the chemical composition (in order to decrease the interval between the stable and metastable equilibrium diagrams), the solidification rate, or both.[7,8] Then, the amount of carbides and matrix microconstituents can be controlled by selecting the chemical composition and heat treatment parameters, respectively.

It should be taken into account that undercooling affects microsegregation. The lower the cooling rate, the greater the microsegregation effect, and so the probability of carbide precipitation at the Last To Freeze (LTF) zones increases and promotes alloyed carbides formation. As a consequence, the size and composition of carbides may vary significantly, from typical unalloyed ledeburitic carbides to high-alloyed carbides,[9–12] depending on the cooling conditions. It has been demonstrated that non alloyed carbides (produced either by controlling the cooling rate or the silicon level) are less stable than high alloyed carbides, and have a high tendency to dissolve during the austenitizing stage of heat treatments.[13,14]

As already mentioned, CADI applications are very recent and mainly linked to agricultural and mining machinery. In certain cases, CADI abrasion resistance can be compared to that of quenched and tempered steels or white cast irons, having the advantage of a lower production cost.[8] Nonethe-

less, the challenge posed by CADI development is obtaining an optimal balance between abrasion resistance and impact toughness for each application.

Dual Phase Austempered Ductile Iron (dual phase ADI). A new type of DI, usually referred to as dual phase ADI, is also under development. The matrix of a dual phase ADI is composed by ausferrite (as in regular ADI microstructure) and free or allotriomorphic ferrite, in an attempt to combine the high tensile strength and toughness of the ausferrite with the high ductility of ferrite.[15–24)]

Different methodologies have been applied to obtain dual phase microstructures.[15–20)] The simplest method seems to be that described by Basso *et al*.[21,22)] and Kilicli *et al*.,[23,24)] which consists of an incomplete austenization stage at temperatures within the intercritical interval, where austenite (γ) ferrite (α) and graphite (Gr) coexist (**Fig. 1**). Then, an austempering stage in a salt bath is carried out to transform the austenite into ausferrite. This heat treatment allows to obtain microstructures with different morphologies and amounts of free ferrite and ausferrite, depending on the intercritical austenitizing temperature (T_{IC}).

Several studies have been conducted to evaluate the influence that variables such as austenitizing temperature ($T\gamma$), austempering temperature (Ta) and part size thickness exert influences on the microstructure and mechanical properties of dual phase ADI.[21,22)] The results indicate that interesting combinations between tensile strength and elongation can be obtained.[19–24)] Fracture toughness tests have also revealed encouraging results when compared to those of fully ferritic or fully ausferritic matrices.[21)]

Multi-Phase Ductile Irons (MPDI). Based on the experience gained when exploring CADI and dual phase ADI, the authors found motivating the possibility of obtaining a new type of DI with a multi-phase microstructure combining the main characteristics of those variants.

The objective of this work is to obtain and characterize the microstructure of this new type of DI with a Multi-Phase Microstructure (MPDI) consisting of free ferrite, ausferrite, free carbides and graphite nodules.

2. Experimental Procedure

2.1. Melt and Sample Preparation

A ductile iron melt was prepared in a medium frequency induction furnace at the laboratory of an industrial foundry plant (Titania S.A. Campana - Argentina). Steel scrap and foundry returns were used as raw materials. The nodularization treatment was conducted using the sandwich method, employing 1.5 mass % of Fe–Si–6 mass %Mg. The melt was inoculated with 0.6 mass% of ferrosilicon (Fe–75 mass %Si), alloyed with chromium to promote free carbides precipitation, and poured into 25 mm thick Y-blocks, from which round samples of 12 mm in diameter and 25 mm in length were cut and used as test specimens.

2.2. Heat Treatments

Taking into account the procedures reported in the literature,[22,23)] in order to determine the characteristic parameters of the intercritical interval, cast samples were first ferritized following an annealing in a muffle furnace, consisting of an austenitizing step at $T\gamma$=900°C for $t\gamma$=3 h, cooling inside the furnace down to 740°C and holding for 10 h. Finally, the samples were cooled down to room temperature inside the furnace.

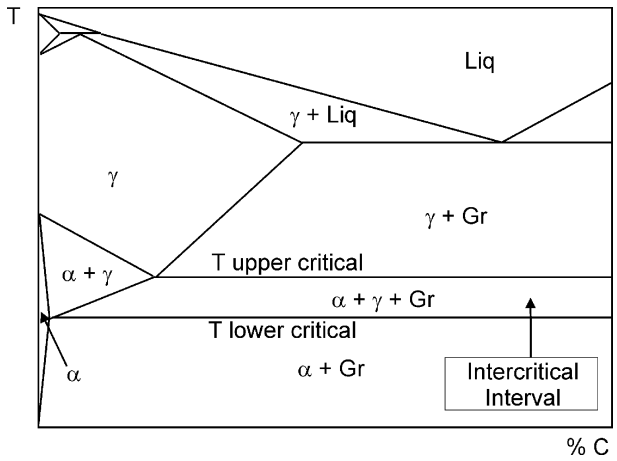

Fig. 1. Schematic pseudo binary Fe–C phase diagram at a constant amount of Si (not in scale).

The upper and lower intercritical temperatures, U_{CT} and L_{CT}, respectively, were determined by using the methodology described in a previous work.[21)] The ferritized samples were heated up to the interval 740–880°C, in steps of 10°C and held at each temperature for 2 h, and then water quenched. The resulting microstructures were composed of different amounts of ferrite (original matrix) and martensite (quenched austenite). The L_{CT} was defined as the temperature at which the first signs of martensite were observed in the quenched samples. The U_{CT}, in turn, was defined as the temperature at which no ferrite was seen in the matrix.

Even though the final objective was to obtain matrices consisting of different amounts of ferrite and ausferrite, it is noteworthy that to determine U_{CT} and L_{CT}, the austempering stage was replaced by water quenching, to use a shorter and easier heat treatment. Thus, a final austenite → martensite reaction was promoted instead of the austenite → ausferrite transformation.

In order to obtain multi-phase microstructures, an austempering step was performed in a salt bath.

2.3. Chemical and Microstructural Studies

The chemical composition of the alloy was determined by means of a Baird spark emission optic spectrometer with a DV6 excitation source. The microstructural characterization was made by optical microscopy. Sample preparation was carried out by using standard techniques for cutting and polishing before etching with 2% Nital. For carbide quantification, the samples were etched with 10% ammonium persulfate in aqueous solution and the content was measured at several random locations of the microstructure with a magnification of 5X. The error for carbide content measurement was estimated in 5%.

The volume fraction of the free carbides, was determined by optical microscopy, using the image Pro Plus software.[25)] The values reported are the average of at least five determinations on each sample. The volume fraction of carbides was measured in both, the as cast and the heat treated conditions, thus allowing to analyze the stability of carbides during the austenization stage.

3. Resuts and Discussion

3.1. Characterization of the As-cast Microstructure

Table 1 lists the chemical composition of the melt, showing its slightly hypoeutectic composition (Equivalent Carbon ~4.1).

The main alloying element introduced was Cr, as a means of promoting alloyed carbides precipitation at the last to freeze regions during solidification. Cu was added in a small quantity to increase austemperability. The microstructure of samples in as cast condition reflected that the original matrix was fully pearlitic (**Fig. 2**). A nodularity of over 90% and a nodule count of ~110 nod/mm^2 were determined in line with the ASTM A247 standard. The free carbides content present in the as cast conditions was of the order of ~15%.

3.2. Microstructural Characterization after Heat Treatments

Table 2 lists the content of free carbide in as-cast and annealed conditions for the central and subsurface regions of the Y- block, revealing that at the central region there is almost no difference between the values measured. The absence of carbide dissolution has been explained in a previous work[13] on the basis of Cr tendency to segregate to the LTF zones, due to the high Cr content in the melt, which increases the thermodynamic stability. Table 2 shows that a small difference exists in the subsurface region when the as-cast and annealed conditions are compared. This was attributed to the lower Cr concentration due to higher cooling rate near the surface of the Y-block, producing less stable alloyed carbides.

Table 1. Chemical composition of the melt (mass %).

C	Si	Mn	Cu	Cr	Mg	P	S	CE
3.2	3.1	0.49	0.3	1.92	0.04	0.02	0.02	4.1

Table 2. Free carbide content (vol. %) in the as-cast condition and after annealing, at the center and near the surface regions of the Y-block.

Condition	Location	
	Center	Near surface
As cast	14	15
Annealed	13	11

After annealing, the metallic matrix of all samples was ferritic with a fine dispersion of small globular carbides, aside from free carbides formed during solidification, as illustrated in **Figs. 3**(a) and (b). Cr presence explained why a complete ferritic microstructure could not be attained.

In order to determine the origin of the small globular carbides, a sample of as cast material was subject to a different annealing heat treatment, which consisted of a complete austenization at 900°C for 3 hours, followed by continuous cooling inside the furnace until room temperature. The result was a microstructure consisting of a continuous ferritic matrix with laminar cementite. Hence it was concluded that the small globular carbides were cementite, which did not dissolve during the 10 hour holding at 740°C in the annealing heat treatment.

3.2.1. Determination of the Intercritical Temperatures L_{CT} and U_{CT}

The L_{CT} and U_{CT} temperatures were determined following the procedure described in Section 2. The first signs of martensite after quenching were observed in the sample heated at 810°C, i.e. L_{CT}, while the fully martensitic structure was noticed in the sample heated at 860°C, thus setting this temperature as the U_{CT}. When comparing these results with those postulated in previous studies,[21,22,26] it is clear that Cr addition has a strong influence on closing the intercritical

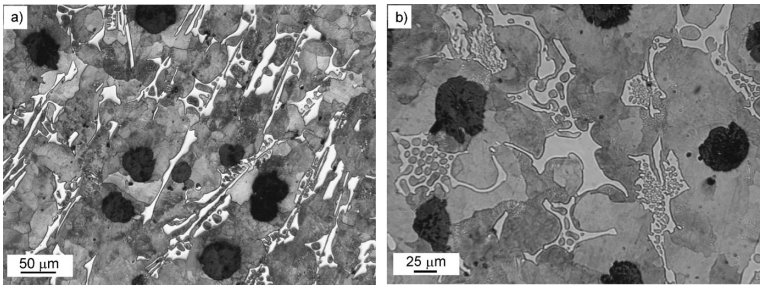

Fig. 2. Microstructures in the as-cast condition at two magnifications, etched with 2% Nital.

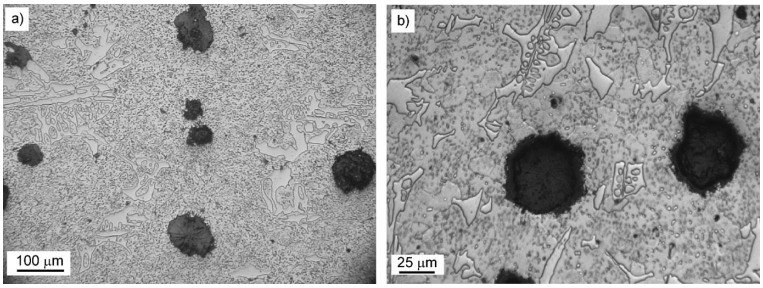

Fig. 3. Microstructures after annealing at two different magnifications, etched with 2% Nital. Annealing conditions: Tγ= 900°C, tγ= 3 h, cooling inside the furnace down to 740°C and holding for 10 h.

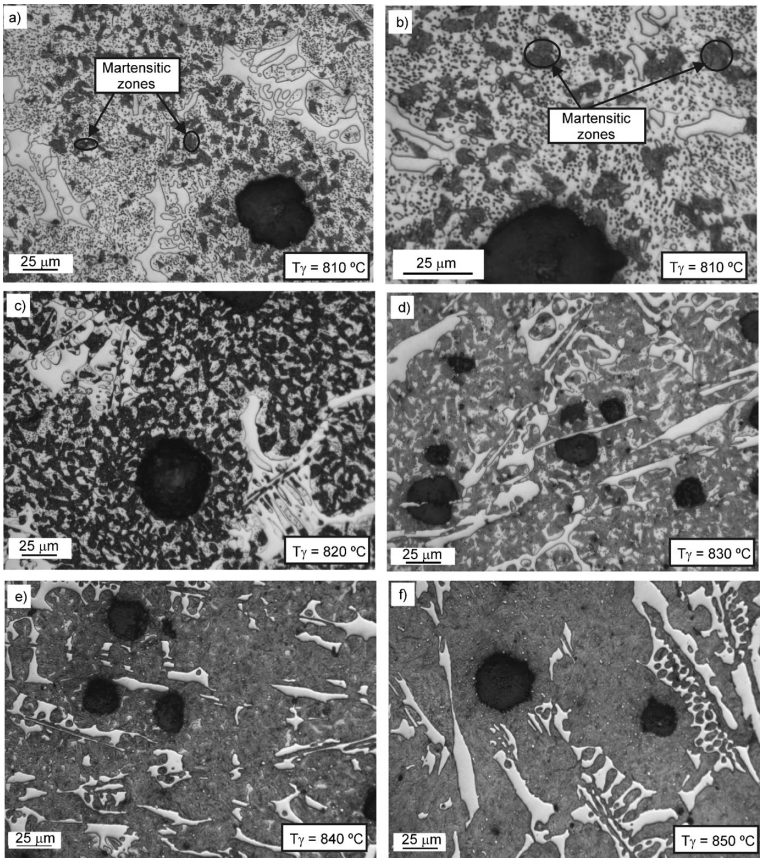

Fig. 4. Microstructures obtained for annealed samples after austenitising for $t\gamma$= 2 h at different temperatures within the intercritical interval: a) and b) $T\gamma$= 810°C, c) $T\gamma$= 820°C, d) $T\gamma$= 830°C, e) $T\gamma$= 840°C, f) $T\gamma$= 850°C; followed by water quenching.

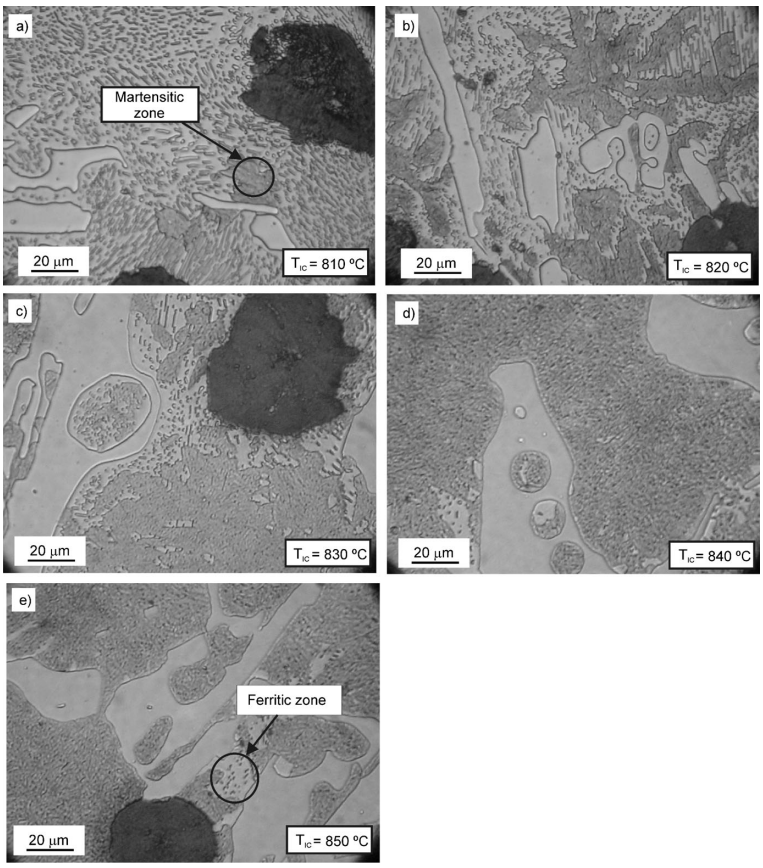

Fig. 5. Microstructures obtained (starting condition as-cast) after heat treatment at different T_{IC} and t_{IC} = 2, followed by water quenching. a) T_{IC} = 810°C, b) T_{IC} = 820°C, c) T_{IC} = 830°C, d) T_{IC} = 840°C, e) T_{IC} = 850°C.

interval by increasing L_{CT} and decreasing U_{CT}. L_{CT} increase was much more notorious than U_{CT} decrease.

Figure 4 depicts the microstructure of five samples austenitized at different Tγ(810, 820, 830, 840 and 850°C) and quenched from the intercritical interval. In all cases, the dark gray regions correspond to martensite and the large white regions to free carbides. In the samples austenitized at Tγ= 810 and 820°C, the other white zones are free ferrite, within which small globular carbides can be observed.

When the austenitizing temperature was close to L_{CT} = 810°C (Figs. 4(a) to 4(c)), the volume fraction of ferrite was higher. Conversely, martensite was the main microconstituent when the temperature was close to U_{CT} = 860°C (Figs. 4(e) and 4(f)). The microstructure obtained at an intermediate austenitizing temperature is shown in Fig. 4(c)).

On the basis of these results, it is worthy of mention that for this alloy, heat treatments involving austenitizing within the intercritical interval followed by quenching led to multi-phase structures, composed of free carbides and different quantities of ferrite and martensite.

3.2.2. Microstructures Obtained from the As-Cast Samples

The technical disadvantage featured by the use of a heat treatment such as the one described above is that it needs annealing. Therefore, the possibility of obtaining similar multi-phase microstructures directly from as cast samples was analyzed.

The phases in thermodynamic equilibrium within the intercritical interval (α+γ+Gr) must be present after a certain holding time at L_{CT}<T < U_{CT} regardless of the starting matrix microstructure. Therefore, the time (t_{IC}) required to reach this thermodynamic equilibrium should be established before analyzing the volume fractions of the phases at each intercritical temperature (T_{IC}). To that end, four samples in as cast condition were held in a furnace at T_{IC}=830°C during t_{IC}=1, 2, 3 and 4 hours, and then they were water quenched.

The volume fractions of martensite and ferrite obtained for the different t_{IC} were exactly the same for all samples, and identical to that of the annealed sample austenitised at 830°C. This means that the pearlite → austenite reaction occurs at high speed. The only difference observed was that by increasing t_{IC}, the remaining cementite derived from the incomplete pearlite → ferrite reaction became more globular.

Once the kinetics of the reaction was defined, as cast bars were heat treated at T_{IC}=810, 820, 830, 840, and 850°C using a holding time of t_{IC}=2 hours each. The resulting microstructures in **Fig. 5** are similar to those in Fig. 4, demonstrating that as T_{IC} increases, the amount of martensite increases too, while the amount of free ferrite decreases. Inside the ferrite areas, a fine dispersion of globulized cementite can be noticed. These results confirm that the multi-phase structures can also be derived from as cast material.

3.2.3. Multi-phase Microstructures Composed of Ausferrite+Ferrite+Carbides

As mentioned above, the objective of this study was to evaluate the possibility of obtaining a new type of DI with a multi-phase microstructure formed by free carbides, allotriomorphic ferrite and ausferrite. Consequently, in order to

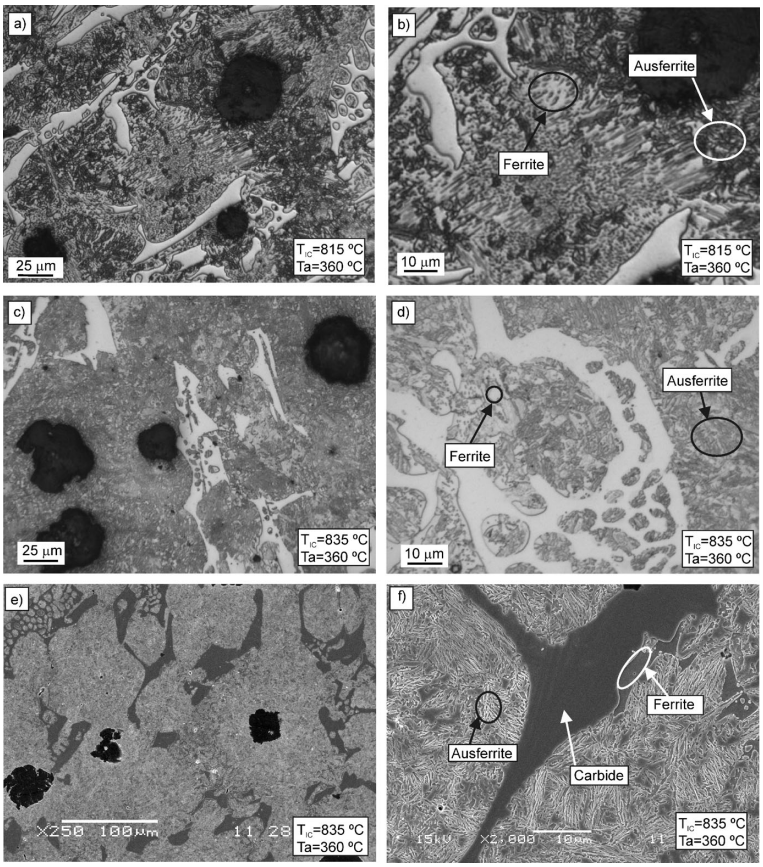

Fig. 6. Multi-phase microstructures obtained in samples austenitised within the intercritical interval and austempered at Ta = 360×C during ta = 90 min; a) and b) T_{IC} = 815°C, t_{IC} = 2 h; c), d), e) and f) T_{IC} = 835°C, t_{IC} = 2 h.

obtain these microstructures, after maintaining at the selected intercritical temperature samples were subjected to an austempering stage, rather than to water quenching. This led to the austenite → ausferrite transformation rather than to the austenite → martensite reaction used in Sections 3.2.1 and 3.2.2.

The microstructures of the austempered samples in **Fig. 6** show that the only difference with those depicted in Figs. 4 and 5 is that martensite has been entirely replaced by ausferrite. Samples austenization and austempering temperatures are indicated in each figure. As it can be seen, the amount of ausferrite is much greater in the microstructure with the higher T_{IC} as it was observed in Figs. 4 and 5 (when the amounts of martensite were compared for different T_{IC}). Figures 6(b), 6(d) and 6(f) are the microstructures at higher magnifications of Figs. 6(a), 6(c) and 6(e), respectively. Figs. 6(e) and 6(f) were obtained using SEM. Ausferrite morphology is clear in Figs. 6(d) and 6(f).

The industrial interest of this new DI lies in the possibility of finding proper combinations of technological properties. This is currently being studied using DI alloyed with different Si and Cr contents.

4. Conclusions

(1) Heat treatments applied to DI alloyed with 2 mass %Cr, involving an incomplete austenitizing stage within the intercritical interval of the Fe–C–Si equilibrium diagram, led to a DI with a microstructure composed of free carbides, free ferrite and ausferrite.

(2) Chromium has a strong effect on the intercritical interval temperatures by notoriously increasing L_{CT}. Thus the interval closes in comparison with similar DI melts without chromium.

(3) With previous annealing, heat treatment allowed to obtain microstructures composed of free carbides (precipitated during solidification), ferrite and different amounts of ausferrite (or martensite) depending on the austenitizing temperature within the intercritical interval. These novel multi-phase structures can also be obtained from as cast material (avoiding previous annealing).

(4) The carbide content present in the final microstructures (after heat treatment) remained mostly unchanged with respect to the amount present in the as cast condition. This was attributed to the high thermodynamic stability of the alloyed carbides formed during solidification, particularly those in the last to freeze zones.

Acknowledgements

The financial support given by CONICET, FONCYT and the National University of Mar del Plata, Mar del Plata, Argentina, is gratefully acknowledged.

REFERENCES

1) K. S. Al-Rubaie: *Wear*, **243** (2000), 92.
2) S. Laino, J. A. Sikora and R. C. Dommarco: *ISIJ Int*., **49** (2009), No. 8, 1239.
3) S. Laino, J. A. Sikora and R. C. Dommarco: *ISIJ Int*., **50** (2010), No. 3, 418.
4) US Patent # 6,258,180 B1, Wear resistant ductile iron, July 2001.
5) ADI Treatments Limited: Furnace is key to CADI solutions, Foundry Trade Journal (2006), 58.
6) S. Laino, J. A. Sikora and R. C. Dommarco: *Wear*, **265** (2008), 1.
7) J. R. Keough and K. L. Hayrynen: *Ductile Iron News*, **3** (2000).
8) K. L. Hayrynen and K. R. Brandenberg: *Am. Foundry Soc*., **111** (2003), 845.
9) R. B. Gundlach, J. F. Janowak, S. Bechet and K. Rohrig: *Mater. Res. Soc. Sympo. Proc.*, **34** (1985), 251.
10) J. Lacaze, G. T. Camacho and C. Bak: *Int. J. Cast Met. Res*., **16** (2003), 167.
11) L. Nastac and D. M. Stefanescu: *Adv. Mater. Res*., **4–5** (1997), 469.
12) H. Zhao and B. Liu: *ISIJ Int*., **41** (2001), 986.
13) M. Caldera, G. Rivera, R. Boeri and J. Sikora: *Mater. Sci. Technol*., **21** (2005), No. 10, 1187.
14) S. Laino, H. R. Ortiz and R. C. Dommarco: *ISIJ Int*., **49** (2009), No. 1, 132.
15) N. Wade and Y. Ueda: *Trans. Iron Steel Inst. Jpn.*, **21** (1981), No. 2, 117.
16) Z. R. He (He Zerong), G. X. Lin and S. Ji: *Mater. Charact.*, **38** (1997), 251.
17) A. Rashidi and M. Moshrefi-Torbati: *Mater. Lett*., **45** (2000), 203.
18) I. Galarreta, R. Boeri and J. Sikora: *Int. J. Cast Met. Res*., **9** (1997), 353.
19) J. Aranzabal, G. Serramoglia and D. Rousiere: *Int. J. Cast Met. Res*., **16** (2002), No. 1, 185.
20) C. Verdu, J. Adrien and A. Reynaud: *Int. J. Cast Met. Res*., **18** (2005), No. 6, 346.
21) A. Basso, R. Martinez and J. Sikora: *Mater. Sci. Technol*., **23** (2007), No. 11, 1321.
22) A. Basso, R. Martinez and J. Sikora: *Mater. Sci. Technol*., **25** (2009), No. 10, 1271.
23) V. Kilicli and M. Erdogan: *Mater. Sci. Technol*., **22** (2006), No. 8, 919.
24) V. Kilicli and M. Erdogan: *Int. J. Cast Met*., **20** (2007), No. 4, 202.
25) Quantitative microscopy. Chapter 3: Measurement of volume in volume, McGraw-Hill Book Company, New York, USA, (1968), **45**.
26) A. Basso, R. A. Martinez and J. A. Sikora: Proc. 8th Int. Symp. on Science and Processing of Cast Iron, Tsinghua University Press, Beijing, China, (2006), 408.